ICHEP 2022 BOLOGNA

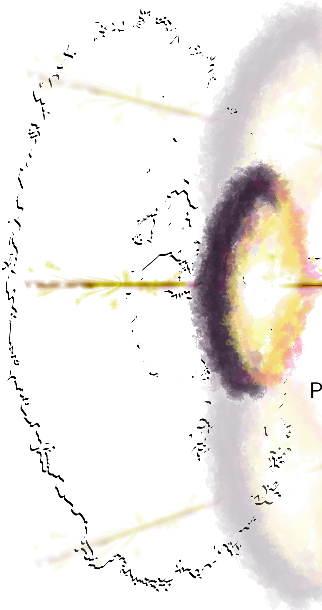

Blazar-Boosted Dark Matter

Talk based on arXiv:2111.13644 and arXiv:2202.07598

Alessandro Granelli
Ph.D. Student in Astroparticle Physics (SISSA)
Collaborators: Jin-Wei Wang and Piero Ullio

SISSA

Direct Detection of Dark Matter

Dark Matter problem

The particle nature of dark matter (DM) is still unknown.

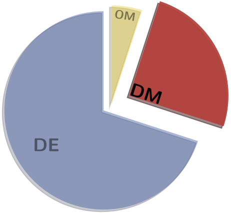

Direct Detection

E.g., XENON1T, designed to detect WIMPs in the local halo. No constraints below $\sim$ 1 GeV.

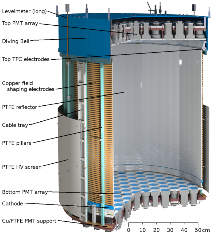

Boosted DM scenarios

E.g., galactic Cosmic Rays (CRs) boosting local DM particle (CRDM scenario) [arXiv:1810.10543].

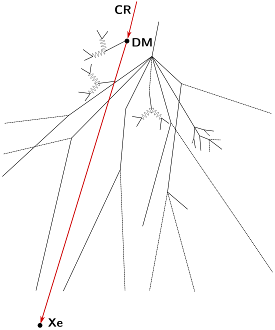

Image Credits: XENON1T from arXiv:2006.09721.

Blazars: Particle Accelerators in the Universe

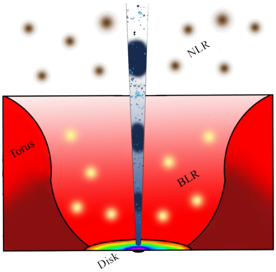

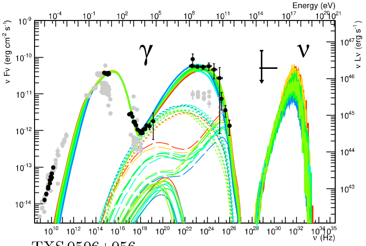

Active Galactic Nuclei

Blazars are AGNs **pointing** (almost) directly **at Earth**.

Supermassive BH

BHs at the center accreting ordinary matter and **focusing DM** particles.

Blazar jets

Emission **of relativistic electrons and protons** as a back-to-back paired jet.

Spectral Energy Distribution (SED) of photons ⇒ info on jet physics. Either Leptonic of Hadronic models.

High-energy neutrinos, e.g. detected at IceCube from TXS 0506+056
⇒ Hadronic component in the jet.

Image Credits: AGN from arXiv:2012.13302, SED from arXiv:1807.04335 (M. Cerruti et al.).

Blazar-Boosted Dark Matter (BBDM)

In arXiv:2111.13644 and 2202.07598 we have investigated the possibility of **protons and electrons in the jet** of a **blazar boosting** the neighbouring **DM particles** to Earth.

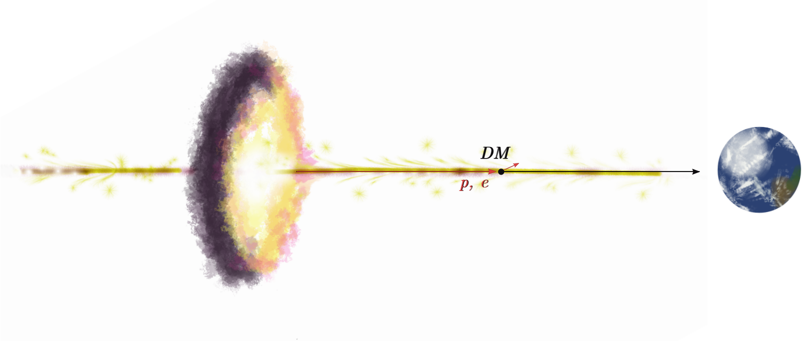

Motivation

A signal can possibly be detected at direct detection or neutrino facilities like **XENON1T**, **Borexino**, **MiniBooNE** and **Super-Kamiokande** (Super-K). The null detection leads to **constraints on** the DM-proton and DM-electron **cross-sections**.

Image Credits: Dr. Veronica Conti (University of Siena).

Blazar-Boosted Dark Matter (BBDM)

Framework – Blazar Jet Model

- We focused on **TXS 0506+056**: high energy neutrinos detected at IceCube. For comparison, BL Lacertae also considered, but (similar) results not reported here.
- We concentrated on hybrid **(lepto-)hardonic models** for the SED (which predict neutrino flux consistent with IceCube observations).
- Single-zone jet model, adopting the **"blob geometry"**: the photon emission originates from a spherical region that moves towards the Earth with speed β_B and Lorentz factor $\Gamma_B = (1-\beta_B^2)^{-1/2}$.
- **Isotropic power-law distribution** for protons and electrons in the "blob frame":

$$\frac{d\Gamma'_j}{dE'_j\, d\Omega'} = \frac{1}{4\pi} c_j \left(\frac{E'_j}{m_j}\right)^{-\alpha_j} \tag{1}$$

  with $j \in \{e,\, p\}$ and $\gamma'_{\mathrm{min},\,j} \leq E'_j/m_j \leq \gamma'_{\mathrm{max},\,j}$.
- The relevant parameters, such as $\gamma'_{\mathrm{min},\,j}$, $\gamma'_{\mathrm{max},\,j}$, Γ_B, α_j, L_j, are fitted from SED observations, and the constant c_j is fixed via:

$$L_j = \int d\Omega \int dT_j\, (T_j + m_j)\, \frac{d\Gamma_j}{dT_j\, d\Omega} = c_j m_j^2 \Gamma_B^2 \int_{\gamma'_{\mathrm{min},\,j}}^{\gamma'_{\mathrm{max},\,j}} d\gamma'_j\, (\gamma'_j)^{1-\alpha_j}\,. \tag{2}$$

(Lepto-)Hadronic Model Parameters		
Parameter (unit)	TXS 0506+056	BL Lacertae
z	0.337	0.069
d_L (Mpc)	1835.4	322.7
M_{BH} ($M_\odot$)	3.09×10^8	8.65×10^7
$\mathcal{D}$	$40^\star$	15
Γ_B	20	15
θ_{LOS} ($^\circ$)	0	3.82
α_p	2.0	2.4
α_e	2.0	3.5
$\gamma'_{\text{min},\,p}$	1.0	1.0
$\gamma'_{\text{max},\,p}$	$5.5 \times 10^{7\star}$	1.9×10^9
$\gamma'_{\text{min},\,e}$	500	700
$\gamma'_{\text{max},\,e}$	$1.3 \times 10^{4\star}$	1.5×10^4
L_p (erg/s)	$2.55 \times 10^{48\star}$	9.8×10^{48}
L_e (erg/s)	$1.32 \times 10^{44\star}$	8.7×10^{42}
c_p ($\text{s}^{-1}\text{sr}^{-1}\text{GeV}^{-1}$)	2.54×10^{47}	1.24×10^{49}
c_e ($\text{s}^{-1}\text{sr}^{-1}\text{GeV}^{-1}$)	2.42×10^{50}	2.59×10^{54}

Table: TXS 0506+056 data from arXiv:1807.04335, BL Lacertae data from arXiv:1304.0605. $'$ In the blob frame. * Mean values.

Jet Spectrum

To get the proton/electron spectrum in the frame of an observer at Earth, we perform a **Lorentz boost** from the blob frame [arXiv:1008.2230]:

$$\frac{d\Gamma_j}{dT_j d\Omega} = \frac{c_j}{4\pi}\left(1+\frac{T_j}{m_j}\right)^{-\alpha_j} \frac{\beta_j(1-\beta_j\beta_B\mu)^{-\alpha_j}\Gamma_B^{-\alpha_j}}{\sqrt{(1-\beta_j\beta_B\mu)^2-(1-\beta_j^2)(1-\beta_B^2)}} \quad (3)$$

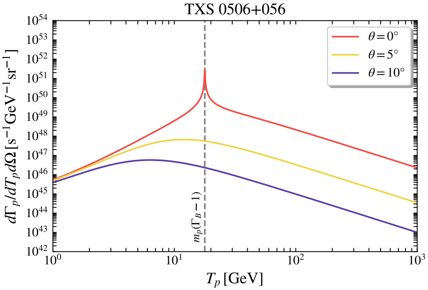

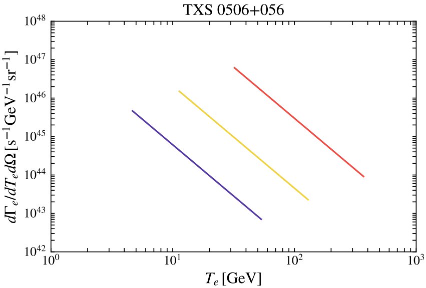

DM profile around the BH

Gondolo & Silk DM Spike

A pre-existent self-gravitating spherical DM profile with power-law scaling $\rho(r) \propto r^{-\gamma}$ is modified into $\rho'(r) \propto r^{-\alpha}$ with $\alpha = -(9-2\gamma)/(4-\gamma)$, [arXiv:astro-ph/9906391], normalised such that [arXiv:astro-ph/0101481]:

$$\int_{4R_S}^{10^5 R_S} dr\, 4\pi r^2 \rho'(r) \simeq M_{\rm BH}\,. \tag{4}$$

We then need to take into account eventual DM annihilations giving a maximal profile $\rho_{\rm core} \simeq m_\chi/(\langle\sigma v\rangle_0\, t_{\rm BH})$, so that:

$$\rho_{\rm DM}(r) = \frac{\rho'(r)\rho_{\rm core}}{\rho'(r)+\rho_{\rm core}}\,. \tag{5}$$

We considered an initial Navarro-Frenk-White profile, i.e. $\gamma = 1$, and three benchmark points:

1. $\langle\sigma v\rangle_0 = 0$, so that $\rho_{\rm core} \to +\infty$ and $\rho_{\rm DM} = \rho'$;
2. $\langle\sigma v\rangle_0 = 10^{-28}\,{\rm cm}^3\,{\rm s}^{-1}$ and $t_{\rm BH} = 10^9$ yr;
3. $\langle\sigma v\rangle_0 = 3\times10^{-26}\,{\rm cm}^3\,{\rm s}^{-1}$ and $t_{\rm BH} = 10^9$ yr;

DM profile around the BH

The quantity that is relevant to compute the BBDM flux is the following line-of-sight (LOS) integral:

$$\Sigma_{\mathrm{DM}}^{\mathrm{tot}} \equiv \int_{r_{\mathrm{min}}}^{10\,\mathrm{pc}} \rho_{\mathrm{DM}}(r')\, dr' \,. \tag{6}$$

Any variation of γ, α and/or r_{min} from the values 1, 7/3 and $4R_S$, respectively, would practically correspond to an intermediate situation between the already considered benchmark points.

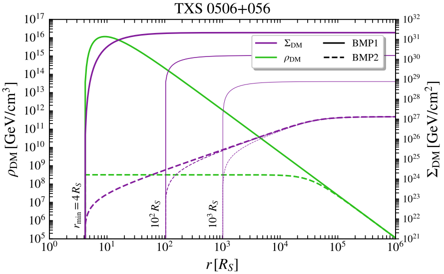

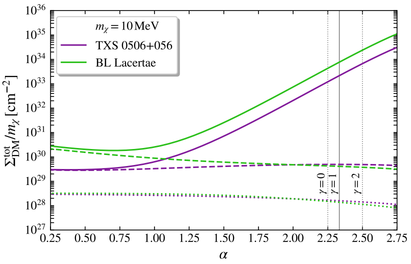

BBDM flux from TXS 0506+056

The BBDM flux at Earth reads:

$$\frac{d\Phi_\chi}{dT_\chi} = \frac{\Sigma_{\rm DM}^{\rm tot}}{m_\chi d_L^2} \sum_{j=e,\,p} \widetilde{\sigma}_{\chi j} \int_{T_j^{\rm min}(T_\chi)}^{T_j^{\rm max}} \frac{dT_j}{T_\chi^{\rm max}(T_j)} \frac{d\Gamma_j}{dT_j d\Omega}\,, \qquad (7)$$

with $\widetilde{\sigma}_{\chi p} = \sigma_{\chi p} G^2(2m_\chi T_\chi/\Lambda_p^2)$, $G(x^2) \equiv 1/(1+x^2)^2$ ($\Lambda_p \simeq 0.77$ GeV) and $\widetilde{\sigma}_{\chi e} \equiv \sigma_{\chi e}$.

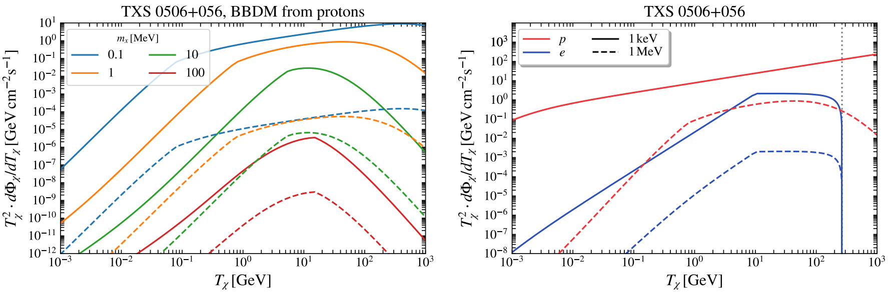

Figure: Left is for $\sigma_{\chi e} = 0$ and $\sigma_{\chi p} = 10^{-30}$ cm^2, right is for $\sigma_{\chi e} = \sigma_{\chi p} = 10^{-30}$ cm^2.

Constraints from Terrestrial Experiments

The expected rate at terrestrial facilities for the scattering of BBDM per target nucleus or electron is (neglecting attenuation):

$$\Gamma_j^{\mathrm{DM}} \simeq \int_{T_{\mathbf{exp}}^{\mathbf{min}}}^{T_{\mathbf{exp}}^{\mathbf{max}}} dT_j\, \widetilde{\sigma}_{\chi j} \int_{T_\chi^{\mathbf{min}}(T_j)}^{+\infty} \frac{dT_\chi}{T_j^{\max}(T_\chi)} \frac{d\Phi_\chi}{dT_\chi} \quad (\text{with } j = e,\, N)\,. \tag{8}$$

Case of $\sigma_{\chi e} = 0$

We impose that the rate is less than the limits from experiments, e.g. for XENON1T, $\Gamma_{\mathbf{Xe}}^{\mathrm{DM}}(4.9 \text{ keV} \leq T_{\mathbf{Xe}} \leq 40.9 \text{ keV}) < 2.41 \times 10^{-34}\ \mathrm{s}^{-1}$. The MiniBooNE experiment instead gives $\Gamma_{\mathbf{p}}^{\mathrm{DM}}(T_p > 35 \text{ MeV}) < 1.5 \times 10^{-32}\ \mathrm{s}^{-1}$. For the spin-dependent case, Borexino sets $\Gamma_{\mathbf{p}}^{\mathrm{DM}}(T_p > 25 \text{ MeV}) < 2 \times 10^{-39}\ \mathrm{s}^{-1}$

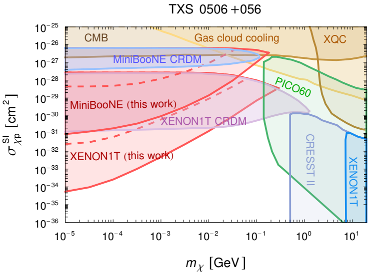

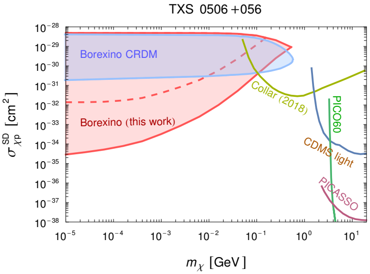

Constraints from Terrestrial Experiments

Case of $\sigma_{\chi e} \neq 0$ at Super-K

With $\sigma_{\chi e} \neq 0$, electron-recoil signals are possible. We studied this using Super-K data from different energy bins presented in arXiv:1711.05278. In this paper, the atmospheric neutrino background is estimated for the various energy bins.

Large volume of Super-K allows to locate the signals. We reduced the background by selecting a proper cone (where more than 95% of the signals are expected) around the source.

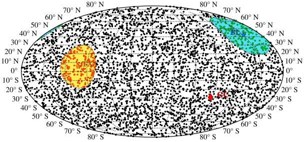

$0.1 < T_e/\text{GeV} < 1.33$
(Bin1)

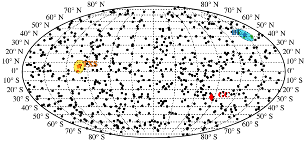

$1.33 < T_e/\text{GeV} < 20$
(Bin2)

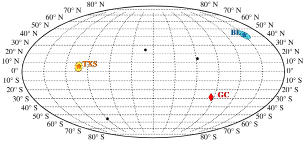

$20 < T_e/\text{GeV} < 10^3$
(Bin3)

Constraints from Terrestrial Experiments

For each bin, the 95% C.L. Poisson limits on the signal rate results to be $\Gamma_e^{DM} < 1.22 \times 10^{-41}\,\mathrm{s}^{-1}$, $2.20 \times 10^{-42}\,\mathrm{s}^{-1}$ and $2.16 \times 10^{-42}\,\mathrm{s}^{-1}$ for Bin1, Bin2 and Bin3, respectively. The corresponding constraints on $\sigma_{\chi e}$ constraints are shown below, compared to CRDM and other limits.

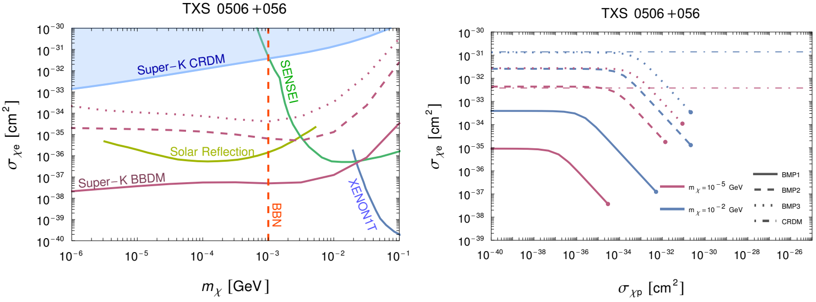

Figure: Left for $\sigma_{\chi p}$ at XENON1T maximal allowed values, right for various $\sigma_{\chi p}$.

Conclusion

Highlights

- **Blazars** are **Ideal DM Boosters**.
- The null detection of BBDM signals at, e.g., XENON1T and Super-K gives very competitive **constraints on** $\sigma_{\chi p}$ **and** $\sigma_{\chi e}$ for $m_\chi \lesssim 1$ GeV.
- This scenario allows to extrapolate more **information on** the **SED jet models** of blazars and/or **DM nature**.

(Some) Future Prospects

- **Improve** the **time correlation study**, e.g. selecting data in better correspondence with blazar flares.
- **Refine** the **direction analysis** of signals, e.g. extract location information at other experimental facilities.
- **Extend** the work **to** the statistical **ensemble of blazars** to reduce model and source selection uncertainties.
- Look at **future** experimental **facilities**, such as DUNE and Hyper-Kamiokande with improved sensitivities.

Thanks for your attention!